Size-controlled synthesis of highly water-soluble silver nanocrystals

Yongxing Hu, Jianping Ge, Donna Lim, Tierui Zhang, Yadong Yin *

Department of Chemistry, University of California, Riverside, CA 92521, USA

ARTICLE INFO

ABSTRACT

We describe a modified polyol process for the synthesis of silver nanocrystals with uniform sizes ranging from several nanometers to ~20 nm. The use of polyacrylic acid, in place of polyvinylpyrrolidone in the conventional polyol process, significantly limits the growth of silver nanocrystals, prevents the interparticle aggregation and fusion, and leads to a uniform population of samples with high water solubility. The size of nanocrystals can be conveniently tuned by controlling the reaction time, the concentration and chain length of the polymeric surfactants, and the reaction temperature. Uniform silver nanocrystals within sizes below 20 nm are preferred candidates over larger particles for applications where high density of optical absorption is required, for example, for photothermal conversion in cancer therapy.

Published by Elsevier Inc.

1. Introduction

The synthesis of silver nanocrystals has been intensively studied for many years mainly because of their unusual optical property as the result of strong localized surface plasmon oscillation [1,2]. Thanks to the high reduction potential of silver cations, a large number of chemical methods have been developed to the preparation of silver nanocrystals with various size, shape and surface properties. Some notable approaches include photo or radiation reduction [3–6], surfactant-assisted reduction in water or other polar solvents [7–10], solvothermal synthesis [11], controlled growth in micelles or microemulsions [12], templating using dendrimers [13], polyol process [14], and thermolysis in nonpolar solvents [15–17]. Very recent progresses have made it possible to produce silver nanocrystals in various shapes ranging from spheres to wires, cubes, plates, prisms, and bipyramids [18–25]. Despite so much success in silver nanocrystal synthesis, interestingly, a careful literature search indicates that there are very few robust approaches capable of producing uniform water-soluble silver nanocrystals with tunable sizes below 20 nm. The well-known polyol process using polyvinylpyrrolidone (PVP) as the surfactant has difficulties to produce silver particles with a narrow size distribution for sizes below ~50 nm. A promising method that can address this size range with narrow size distribution involves the thermolysis of silver salt in nonpolar

solvents [15–17]. However, the hydrophobic surfaces of the products practically limit their applications, particularly in biological systems where water solubility is one of the prerequisites. Additional steps of surface modification are generally required to transfer the hydrophobic nanoparticles to water [26–28].

In this paper, we report that a simple modification to the traditional polyol process can produce highly water-soluble silver nanocrystals with uniform and tunable sizes from several nanometers to ~20 nm. Silver nanocrystals within this size range have some different properties from those larger ones, for example, their extinction spectra are mainly contributed by absorption, while significant scattering occurs for larger particles [29]. The higher density of absorbed energy for small silver nanocrystals may make them preferred candidates for applications such as photothermal therapy [30–32]. The key improvement in our synthesis is to use polyacrylic acid (PAA) instead of traditionally used PVP as the surfactant to direct the growth of silver nanocrystals. Comparing to PVP, PAA shows stronger size-limiting effect due to the higher coordination power of carboxylate groups to silver particle surfaces. In addition, uncoordinated carboxylate groups extend into the aqueous solution, conferring upon the particles a high degree of dispersibility in water [33–35], and also providing abundant anchoring points for further attachment of biomolecules through the well-developed bioconjugation chemistry [36,37]. It has also been noticed that the growth of silver nanocrystals in the presence of PAA follows a simple monomer-addition growth model which is different from the coagulation model in the PVP case. This finding allows

* Corresponding author.
E-mail address: yadong.yin@ucr.edu (Y. Yin).

convenient size control by taking advantage of concepts developed previously for the thermolytic growth of hydrophobic colloidal nanocrystals in nonpolar organic solvents [38].

2. Experimental section

2.1. Chemicals and materials

Silver nitrate (AgNO$_3$, 99+%), short-chain PAA powder (M_w = 1800), and long-chain PAA aqueous solution (M_w = 50,000, 25%) were purchased from Sigma-Aldrich. Ethylene glycol (EG, 99+%) and Triethylene glycol (TEG, 99%) were obtained from Acros Organics. Diethylene glycol (DEG, reagent grade) was purchased from Fisher Scientific. All reagents were used without further purification.

2.2. Synthesis of Ag nanocrystals

Silver nanocrystals with various sizes were synthesized using a modified polyol process, by reducing AgNO$_3$ at the boiling temperature of the solvent. Polyols such as EG, DEG, and TEG were used as the solvent as well as the reducing agent. PAA was used as a surfactant for controlling the growth of silver nanocrystals. In a typical synthesis, AgNO$_3$ (0.1 g) dissolved in EG (3 ml) at room temperature was quickly injected into a boiling solution of EG (15 ml) and PAA (0.030 M) with vigorous stirring under a protective nitrogen atmosphere. Aliquots were extracted using a needle at various times after the injection of precursor solution. Samples were cooled to room temperature, cleaned three times by precipitation with excessive distilled water followed by centrifugation at 11000 rpm, and finally re-dispersed in distilled water by neutralization of the surface carboxylic acid groups with dilute NaOH solution.

2.3. Characterization

Morphology and size distribution of the products were characterized using a Tecnai T12 transmission electron micro-scope (TEM). High-resolution TEM (HRTEM) images were obtained using a Tecnai G2 S-Twin electron microscope operated at 200 kV. The nanocrystals dispersed in water were cast onto a carbon-coated copper grid, followed by evaporation under vacuum at room temperature. The size distribution of the nanoparticles was obtained by measuring over 250 units for each sample. Crystal structures were measured on a Bruker D8 advance X-ray diffractometer (XRD) with a Cu$K\alpha$ radiation (λ = 1.5418 Å). The data were collected from 2θ = 30–70° at a scan rate of 1.5 s per point. The absorption spectrum of an aqueous dispersion of silver nanocrystals was measured by an Ocean Optics HR2000CG-UV–NIR spectrometer.

3. Results and discussion

In a traditional polyol process, metal cations are reduced by polyols such as EG at an elevated temperature. PVP has been extensively used in this process as the surfactant to control the growth of metal particles and prevent their agglomeration. Due to the weak coordination of pyrrolidone to metal surface, a polyol process usually results in metal particles with relatively large size [39]. As shown in a typical example in Fig. 1A, the polyol reduction of silver cations in the presence of PVP leads to particles with typical sizes ranging from 50 nm to above 100 nm [40,41]. Also, the products usually have a broad size distribution and nonuniform shapes if no additional means of control is applied. This is because the formation of silver particles does not strictly follow the classic LaMer model in which nucleation results from the supersaturation of monomers produced by chemical reactions of precursors, and the further growth of particles is realized by absorbing the newly formed monomers. Our observation indicates that with PVP as the only growth directing agent, interparticle aggregation and fusion occur during the later stage of the reaction, which can be clearly observed in Fig. 1A with some dimeric nanocrystals marked by arrows. Therefore, the final products are highly polycrystalline particles containing large amount of defects such as twin planes.
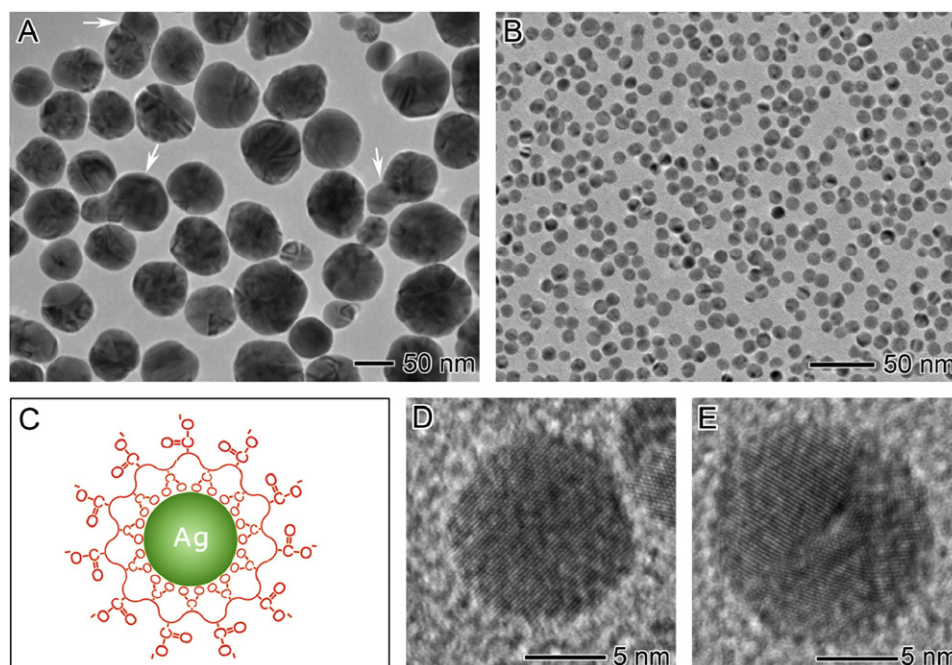

Fig. 1. (A) Silver nanocrystals produced by traditional polyol process using PVP as the surfactant. The coagulation of growing particles results in polycrystalline products as indicated by the arrows. (B) A representative TEM image showing the uniform silver nanocrystals produced through the modified polyol process using PAA as the surfactant. (C) Schematic illustration of a PAA-coated silver nanocrystal. (D, E) HRTEM images of silver nanocrystals (D) without and (E) with defects.

The major modification in the current approach is to use PAA to replace widely used PVP as the surfactant. The coordination of carboxylate to silver surface is much stronger than that of PVP so that PAA can effectively limit the growth of nanocrystals and prevent the aggregation and fusion between the growing particles (Fig. 1B). An additional benefit of using PAA as surface ligand is that the uncoordinated carboxylate groups on the polymer chains provide the products excellent water solubility as well as conjugation sites for convenient attachment of biomolecules. Fig. 1C schematically illustrates the surface structure of the silver nanocrystals synthesized using PAA as the surfactant.

The use of PAA in place of PVP as the surfactant significantly changes the growth mechanism of the silver particles. In the current system, silver nanocrystals grow exclusively by incorporating additional monomers continuously produced in the reaction medium—a typical mechanism that has been found in many colloidal nanocrystal systems such as the well-known case of CdSe quantum dots. Therefore, a number of important strategies that we have learned from those prototypical systems can be used here to produce silver nanocrystals with controlled size and size distributions. For example, it is highly desirable to separate nucleation from growth to produce monodisperse samples. This can be achieved through a rapid injection of precursors into a high-temperature solvent. In addition, a narrow size distribution is favored by a sufficiently high concentration of monomers. This can be achieved by increasing the reaction temperatures and the concentration of precursors. All these strategies have been applied to the modified process. In a typical synthesis, a solution of EG containing the surfactant of PAA is heated up to its boiling temperature under the protection of N_2 flow. A concentrate solution of $AgNO_3$ in EG is rapidly injected into the boiling mixture under vigorous stirring. The solution changes color from clear and colorless at the time of mixing, through light brown, and eventually to dark brown. Fig. 1B shows a typical transmission electron microscopy (TEM) image of uniform silver nanocrystals produced using this modified polyol process. Close inspection with HRTEM indicates that most of the silver particles are single crystals (Fig. 1D), although a small portion of them still contain defects (Fig. 1E).

The nucleation and growth of the silver nanocrystals have been found sensitive to a number of factors, including the reaction temperature and time, the molecular weight and concentration of the surfactant, and the reducing power of the polyol solvent. Therefore, it is possible to produce uniform silver nanocrystals with variable sizes from ~4 to 20 nm by simply changing these reaction conditions. TEM images in parts A–C in Fig. 2 show the evolution of silver nanocrystals at different reaction stage after injecting the precursor in the presence of 0.030 M short-chain PAA ($M_w = 1800$). Nucleation starts at ~4 min after the injection of precursor, as indicated by the sudden change of the solution color from colorless to light brown. Samples harvested right after the color change have an average size of ~4.0±1.2 nm, as shown in Fig. 2A. The initial small particles have a broad size distribution probably due to both the relatively long initiation time for nucleation and the uneven sample extraction during the quick-changing nucleation stage. As the reaction proceeds, the solution color rapidly shifts from light brown to dark brown. TEM image of the sample extracted at ~6 min after the injection of precursor shows significantly increased size with a relatively narrower size distribution (~9.2±1.3 nm), as displayed in Fig. 2B. Compared with the particles in Fig. 2A, the nanocrystals extracted at this stage have more regular spherical shapes. The further growth of the silver particles becomes much slower, as partially suggested by the stable solution color. As shown in Fig. 2C, the sample obtained at ~15 min after the initial injection has a slight increase in average size to ~10±1.7 nm, while maintaining a similar size distribution to the one collected at 6 min.

It has also been found convenient to control the size of the silver nanocrystals by changing the concentration of the polymer surfactant: the size of the nanocrystals decreases with an increase in the concentration of PAA. Parts D–F in Fig. 2 show typical TEM images of silver nanocrystals synthesized in a condition similar to that in parts A–C except for the increased concentration of PAA for three times. As shown in Fig. 2D, the particles collected right after the color change have an average size of 3.5±0.9 nm. The higher concentration of PAA effectively limits the fast growth of silver nanocrystals, resulting in a relatively smaller size, narrower size distribution, and more regular spherical shape than those synthesized with less surfactant. Continued growth for another 2 min greatly increases the size of the particles to ~8.5±1.4 nm, as shown in Fig. 2E. Again, further heating of the system does not have a significant effect on the average size and size distribution of the products. Nanocrystals extracted at ~15 min after the injection of precursor have an average size of ~9.1±1.5 nm, which is slightly smaller than that of the sample produced with less surfactant under otherwise similar conditions.

In principle, the size of nanocrystals can be widely tuned by simply changing the concentration of surfactants. However, this is not always a practical way for size control since the concentration of surfactants affects the rates of both nucleation and growth. A too high concentration may greatly delay the nucleation thus leads to a broad distribution of the final products. On the other hand, a too low concentration may not be able to effectively control the growth and again results in a nonuniform population of particles. For example, the samples prepared by using a reduced concentration of PAA (0.015 M) show very broad distributions at both the early and final stage of the reactions.

Interestingly, the use of PAA with longer chains ($M_w = 50,000$) allows the controllable production of silver nanocrystals with larger average sizes. As shown in Fig. 3, uniform silver nanocrystals of ~14.2±1.7, 15.3±1.7, and ~19.5±2.1 nm can be conveniently produced by simply decreasing the concentration of these long-chain PAA from 2.8×10^{-3} to 1.1×10^{-3} M, and to 5.6×10^{-4} M. The size distribution does not significantly broaden as the average diameter increases. On the other hand, the use of long-chain surfactant at a concentration much higher than 2.8×10^{-3} M leads to the formation of slightly smaller particles; however, the products typically have broad size distributions. Therefore, PAA surfactants with short and long chains work complementary in controlling the size and size distribution of the silver nanocrystals: the short-chain PAA produces smaller nanocrystals at relatively high surfactant concentration while the long-chain PAA works optimally at a lower concentration for forming larger nanocrystals. The weaker size-limiting effect of the long-chain surfactant might be attributed to its lower availability of binding groups resulting from its bulkier chain.

As demonstrated in Fig. 2, it is possible to collect small nanocrystals by stopping the reaction at their early stage of growth. However, the yield of such process is usually low as precursors are only partially converted into nanocrystals. Also, it is practically inconvenient to extract a large amount of sample within a short time frame to ensure a uniform size distribution. To enable the access to small nanocrystals while maintaining the high production yield and narrow size distribution, we further modify the process by increasing the reaction temperature. More nuclei can be produced if the reaction can be initiated at a higher temperature, thus leading to the reduced average size of the products if the amount of starting precursor is kept the same. A high reaction temperature may also favor the production of nanocrystals with a narrow size distribution since nucleation and growth steps can be well-separated at a high reaction rate. In the current system, a higher reaction temperature can be achieved using polyols with longer chains, for example, DEG (b.p.~245 °C)
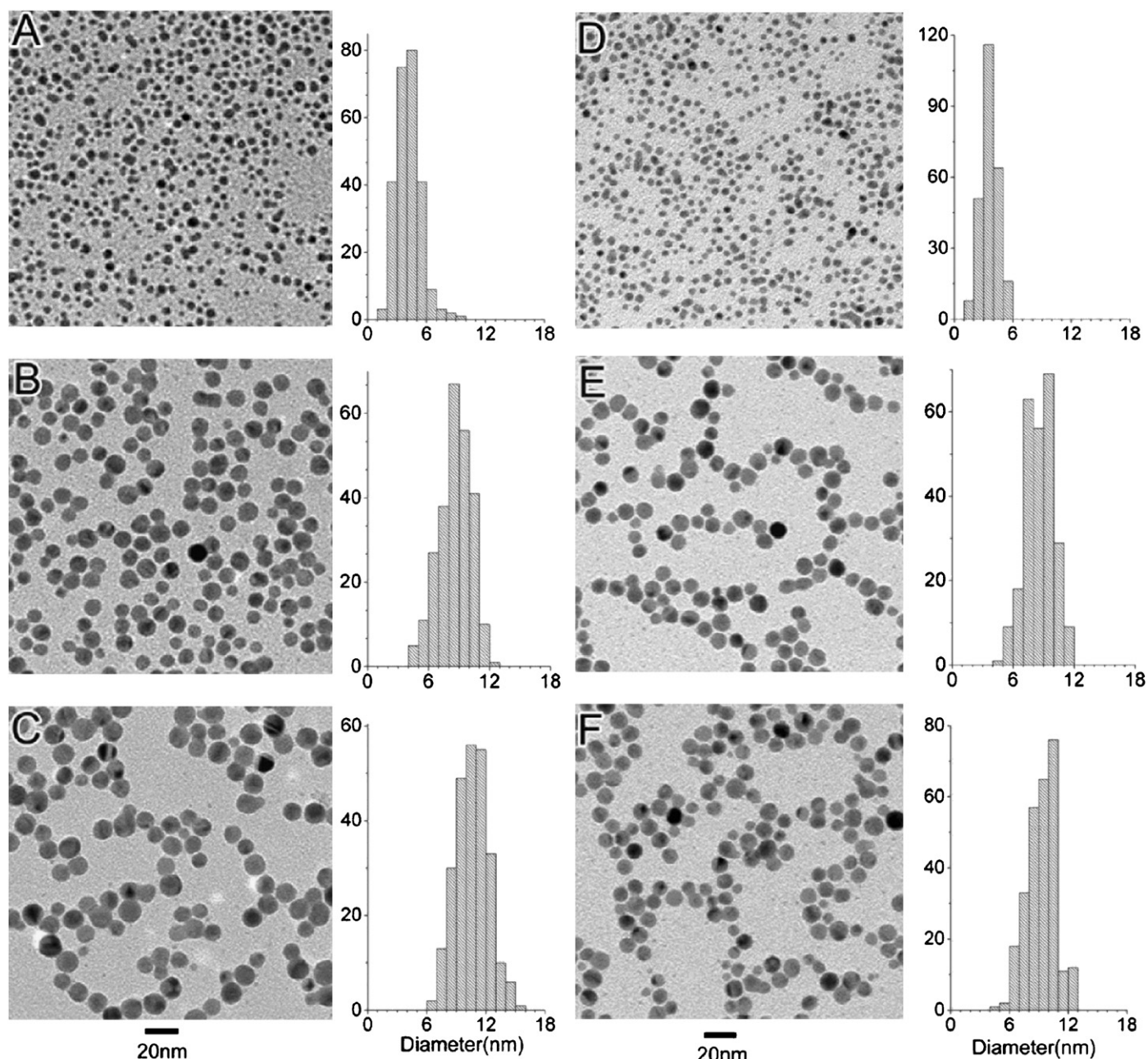
Fig. 2. TEM images and the corresponding size distribution histograms of silver nanocrystals obtained at different stages of the reaction: (A) 4 min, (B) 6 min, and (C) 15 min in the presence of 0.030 M short-chain PAA; and (D) 4 min, (E) 6 min, and (F) 15 min in the presence of 0.090 M short chain PAA.

and TEG (b.p.~285 °C). As shown in Fig. 4A, the initiation time required after injection of precursor to boiling DEG or TEG is of seconds, much shorter than that of EG under similar conditions, indicating much higher reaction rates at higher reaction temperatures. Uniform nanocrystals of 5.4 ± 0.8 and 6.2 ± 1.0 nm were obtained after the reactions have proceeded for ~10 min in boiling DEG and TEG, respectively. Further heating of the samples for another 5 min does not significantly change the size of the products, suggesting that the growth of the nanocrystals has already been close to completion. From parts B and C in Fig. 4, one can see not only the narrow size distribution, but also the greatly reduced size in comparison to that of silver nanocrystals synthesized in EG under similar conditions. Interestingly, the final nanocrystal size obtained from DEG is slightly smaller than

that from TEG although the latter has a higher boiling temperature. Other factors such as the miscibility of the precursor and surfactant with the solvent, instead of the absolute nucleation rates, may contribute to the slight size variation.

XRD measurements have also been performed to reveal the crystal structure of the synthesized samples. Fig. 5 shows the diffraction patterns of nanocrystals prepared using PVP and PAA as surfactants. For all the samples, the three diffraction peaks above 37° correspond to silver (111), (200) and (220) reflections, clearly suggesting the formation of metallic silver with face centered cubic structure (lattice parameter $a = 4.086$ Å). The nanocrystals synthesized in the presence of PVP show very sharp peaks, indicating the large size of the crystals. The full-widths at half-maximum (FWHM) of the diffraction peaks of PAA-stabilized
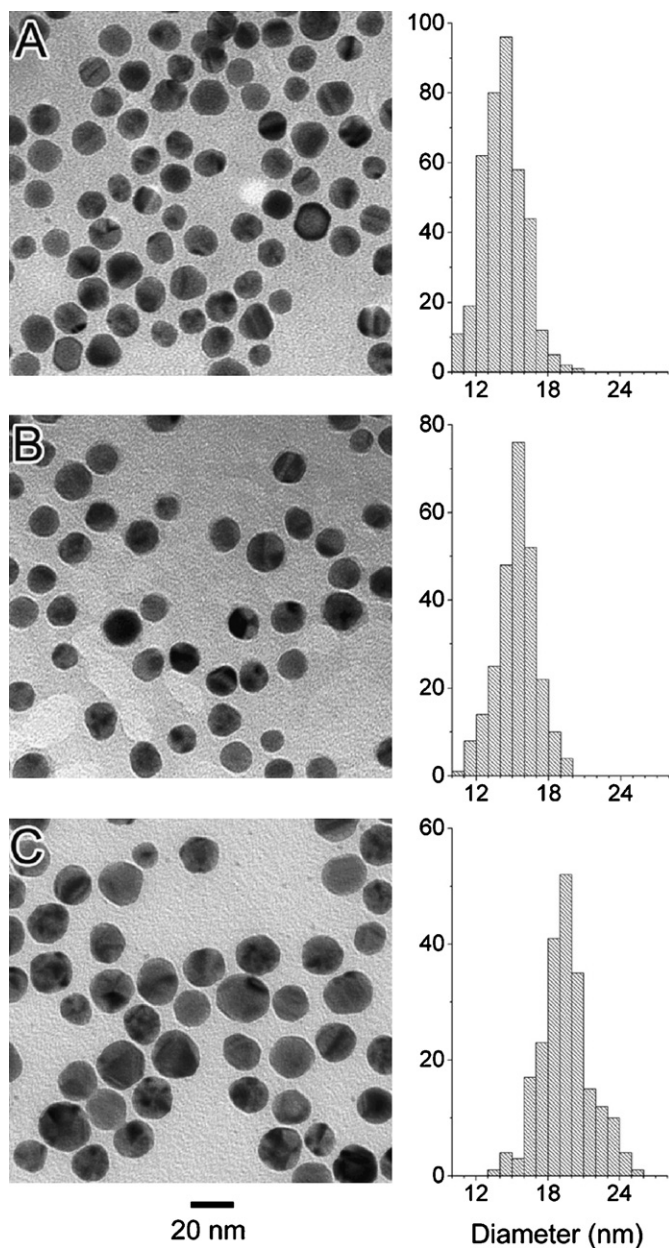
Fig. 3. TEM images and the corresponding size distribution histograms of silver nanocrystals synthesized in the presence of long-chain PAA with concentrations of (A) 2.8×10^{-3} M, (B) 1.1×10^{-3} M, and (C) 5.6×10^{-4} M.

Fig. 4. (A) The initiation time from the injection of precursor to the solution color change required for solvents of EG, DEG and TEG. The solutions were heated at their boiling points. (B) and (C) TEM images of uniform silver nanocrystals produced with 0.030 M short-chain PAA in boiling (B) DEG and (C) TEG after the reactions have proceeded for ~10 min.

samples are significantly broader than that of the PVP-stabilized one, in agreement with the smaller grain sizes in the former cases. One can also notice that the PAA-stabilized nanocrystals synthesized in DEG show relatively lower diffraction intensity and more peak broadening than those in EG. This is also consistent with the fact that nanocrystals synthesized in DEG are smaller.

As the result of strong surface plasmon resonance, the silver nanocrystals produced by using PAA as surfactants show bright yellow color when they are dispersed in water. On the other hand, the particles synthesized in the presence of PVP show grayish color, indicating their broad size distribution as well as the strong scattering of the particles. Fig. 6 shows a typical UV–vis absorption spectrum of the aqueous solution of PAA-stabilized silver nanoparticles prepared in EG. An intense absorption peak at around 400 nm was observed and attributed to the excitation of surface plasma resonance of spherical silver nanocrystals [42–44].
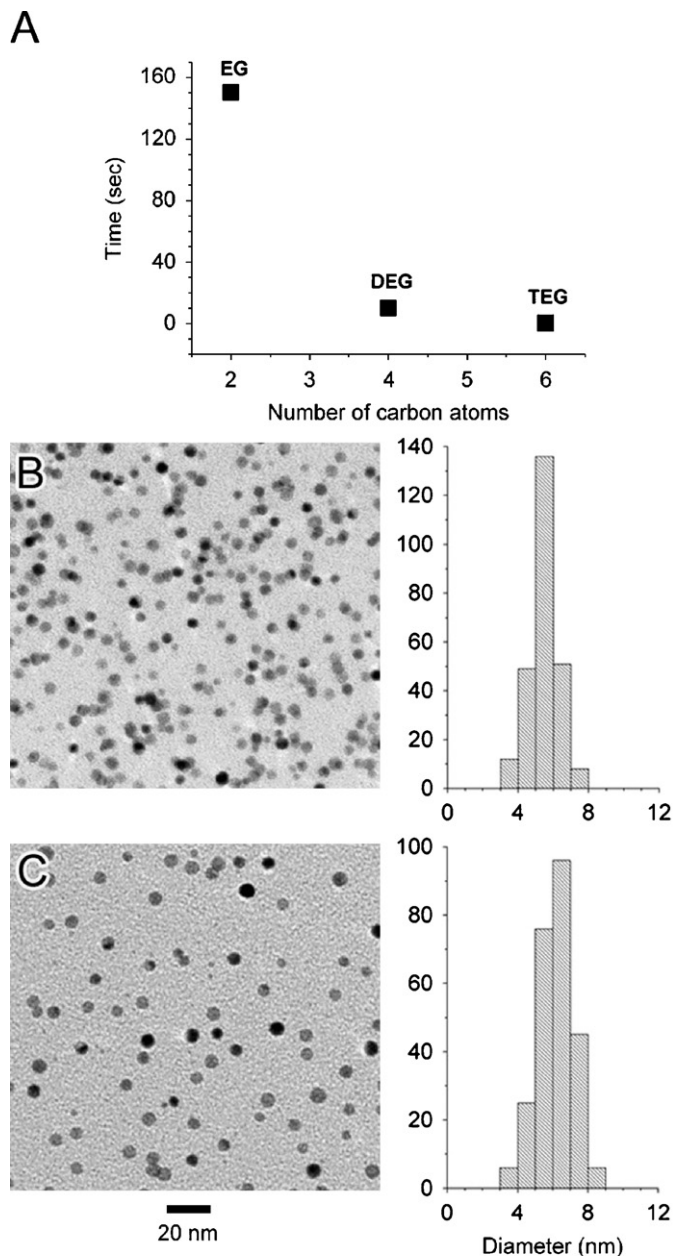
4. Conclusion

The strong coordination of carboxylate groups to silver surface makes PAA an ideal surfactant for polyol process for the controlled synthesis of silver nanocrystals with sizes below 20 nm. The prevention of interparticle aggregation and fusion allows the nanocrystals to grow by following the classic monomer-addition model so that a number of strategies learned from other systems can be used to control the size and size distribution of silver nanocrystals. As a result, the described modification to the conventional polyol process produces silver nanocrystals with uniform and tunable sizes below 20 nm. With the possibility to extend to other metals, the described procedure may greatly
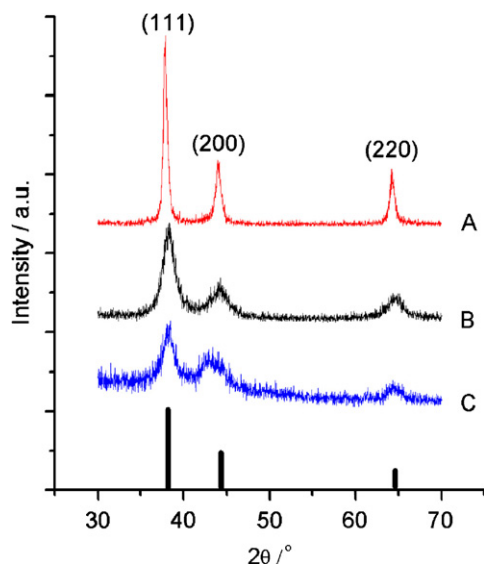
Fig. 5. XRD patterns for silver nanocrystals prepared with (A) PVP in EG, (B) PAA in EG, and (C) PAA in DEG. Peak positions and relative intensities recorded in the literature are indicated by the vertical bars.
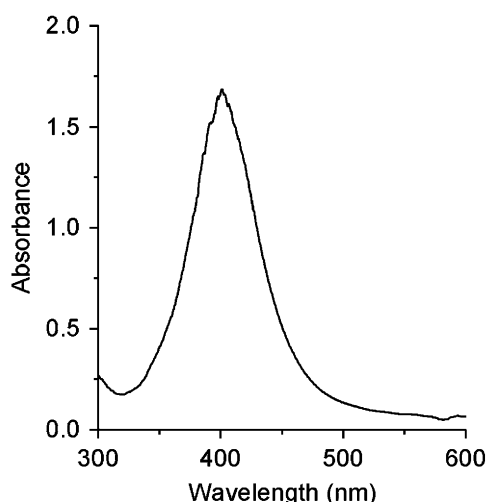

Fig. 6. Typical UV–vis absorption spectrum of an aqueous solution of silver nanocrystals synthesized in the presence of short-chain PAA with concentration of 0.030 M in EG.

improve the applicable scope of the polyol process in the synthesis of nanostructured materials by expanding their sizes to truly nanometer dimensions.

References

[1] A.J. Haes, C.L. Haynes, A.D. McFarland, G.C. Schatz, R.P. van Duyne, S. Zou, MRS Bull. 30 (2005) 368.
[2] E. Hutter, J.H. Fendler, Adv. Mater. 16 (2004) 1685.
[3] A. Henglein, Chem. Mater. 10 (1998) 444.
[4] Y. Yin, X. Xu, C. Xia, X. Ge, Z. Zhang, Chem. Commun. (1998) 941.
[5] A. Henglein, M. Giersig, J. Phys. Chem. B 103 (1999) 9533.
[6] P.L. Redmond, X. Wu, L. Brus, J. Phys. Chem. C 111 (2007) 8942.
[7] T.W. Roberti, B.A. Smith, J.Z. Zhang, J. Chem. Phys. 102 (1995) 3860.
[8] I. Sondi, D.V. Goia, E. Matijevic, J. Colloid Interface Sci. 260 (2003) 75.
[9] L.M. Liz-Marzan, I. Lado-Tourino, Langmuir 12 (1996) 3585.
[10] Y. Yin, Z.-Y. Li, Z. Zhong, B. Gates, Y. Xia, S. Venkateswaran, J. Mater. Chem. 12 (2002) 522.
[11] X. Wang, J. Zhuang, Q. Peng, Y. Li, Nature 437 (2005) 121.
[12] A. Taleb, C. Petit, M.P. Pileni, Chem. Mater. 9 (1997) 950.
[13] M. Zhao, R.M. Crooks, Chem. Mater. 11 (1999) 3379.
[14] S. Ayyappan, G.N. Subbanna, R.S. Gopalan, C.N.R. Rao, Solid State Ion. 84 (1996) 271.
[15] X.Z. Lin, X. Teng, H. Yang, Langmuir 19 (2003) 10081.
[16] Y. Yin, C. Erdonmez, S. Aloni, A.P. Alivisatos, J. Am. Chem. Soc. 128 (2006) 12671.
[17] Y. Lu, G.L. Liu, L.P. Lee, Nano Lett. 5 (2005) 5.
[18] H. Hiramatsu, F.E. Osterloh, Chem. Mater. 16 (2004) 2509.
[19] S. Chen, D.L. Carroll, Nano Lett. 2 (2002) 1003.
[20] K.K. Caswell, C.M. Bender, C.J. Murphy, Nano Lett. 3 (2003) 667.
[21] I. Pastoriza-Santos, L.M. Liz-Marzan, Nano Lett. 2 (2002) 903.
[22] B. Wiley, T. Herricks, Y. Sun, Y. Xia, Nano Lett. 4 (2004) 1733.
[23] Y. Sun, Y. Xia, Science 298 (2002) 2176.
[24] R. Jin, Y. Cao, C.A. Mirkin, K.L. Kelly, G.C. Schatz, J.G. Zheng, Science 294 (2001) 1901.
[25] B. Wiley, Y. Xiong, Z. Li, Y. Yin, Y. Xia, Nano Lett. 6 (2006) 765.
[26] Y. Wang, J.F. Wong, X. Teng, X.Z. Lin, H. Yang, Nano Lett. 3 (2003) 1555.
[27] W.W. Yu, E. Chang, C.M. Sayes, R. Drezek, V.L. Colvin, J. Nanotech. 17 (2006) 4483.
[28] J. Xie, S. Peng, N. Brower, N. Pourmand, S.X. Wang, S. Sun, Pure Appl. Chem. 78 (2006) 1003.
[29] I.O. Sosa, C. Noguez, R.G. Barrera, J. Phys. Chem. B 107 (2003) 6269.
[30] G. Huttmann, R. Birngruber, IEEE J. Sel. Top. Quant. Electron. 5 (1999) 954.
[31] L.R. Hirsch, R.J. Stafford, J.A. Bankson, S.R. Sershen, B. Rivera, R.E. Price, J.D. Hazle, N.J. Halas, J.L. West, PNAS 100 (2003) 13549.
[32] D. Pissuwan, S.M. Valenzuela, M.B. Cortie, Trends Biotechnol. 24 (2006) 62.
[33] J. Ge, Y. Hu, M. Biasini, W.P. Beyermann, Y. Yin, Angew. Chem. Int. Ed. 46 (2007) 4342.
[34] J. Ge, Y. Hu, M. Biasini, C. Dong, J. Guo, W.P. Beyermann, Y. Yin, Chem. Eur. J. 13 (2007) 7153.
[35] T. Zhang, J. Ge, Y. Hu, Y. Yin, Nano Lett. 7 (2007) 3203.
[36] G.T. Hermanson, Bioconjugate Techniques, Academic Press, San Diego, CA, 1996.
[37] R.E. Bailey, S. Nie, in: C.N.R. Rao, A. Müller, A.K. Cheetham (Eds.), The Chemistry of Nanomaterials: Synthesis, Properties and Applications, WILEY-VCH Verlag GmbH & Co. KGaA, Weinheim, 2004, p. 405.
[38] Y. Yin, A.P. Alivisatos, Nature 437 (2005) 664.
[39] F. Fievet, J.P. Lagier, B. Blin, B. Beaudoin, M. Figlarz, Solid State Ion. 32–33 (1989) 198.
[40] M. Figlarz, C. Ducamp-Sanguesa, F. Fievet, J.-P. Lagier, Adv. Powder Metall. 1 (1992) 179.
[41] B. Wiley, Y. Sun, J. Chen, H. Cang, Z.-Y. Li, X. Li, Y. Xia, MRS Bull. 30 (2005) 356.
[42] A. Liebsch, Phys. Rev. B 48 (1993) 11317.
[43] H.H. Huang, X.P. Ni, G.L. Loy, C.H. Chew, K.L. Tan, F.C. Loh, J.F. Deng, G.Q. Xu, Langmuir 12 (1996) 909.
[44] Y. Yin, Z.-Y. Li, Z. Zhong, B. Gates, Y. Xia, S. Venkateswaran, J. Mater. Chem. 12 (2002) 522.